

- magnitude less per pixel than for the DI HRI-IR passively cooled spectrometer, resulting in SST spectra taken at 0.75 AU from the comet with precisions rivaling those obtained by the HRI-IR, taken at 1000 km (6.8×10^{-6} AU) from the comet.
7. C. M. Lisse *et al.*, *Astrophys. J. Lett.* **625**, L139 (2005a).
 8. C. M. Lisse *et al.*, *Space Sci. Rev.* **117**, 161 (2005b).
 9. J. Crovisier *et al.*, *Science* **275**, 1904 (1997).
 10. E. Lellouch *et al.*, *Astron. Astrophys.* **339**, L9 (1998).
 11. K. Malfait *et al.*, *Astron. Astrophys.* **332**, L25 (1998).
 12. D. E. Harker *et al.*, *Science* **310**, 278 (2005).
 13. As a test of the robustness of our best-fit model, the last column in Table 2 also gives the best-fitting χ^2_{ν} , we could find if we deleted a particular species while keeping the rest.
 14. E. Anders, N. Grevesse, *Geochim. Cosmochim. Acta* **53**, 197 (1989).
 15. H is very deficient, as expected for small primitive bodies' inability to retain solar nebula H_2 . C is deficient by a factor of 10, due to its majority partitioning into the comet's labile icy volatiles (CH_4 , C_2H_6 , CO, and CO_2). E. K. Jessberger *et al.* (53) found a C/Mg ratio (atom/atom) in 79 selected large particles during the flythrough of the coma of 1P/Halley that was an order of magnitude greater than in typical IPDs. O is less deficient than C, depleted by only a factor of ~ 2 , due to its more lithophilic chemistry and majority presence in the relatively involatile H_2O . S appears deficient by a factor of 1.5, suggesting that we may not have well characterized the sulfide constituents or that a significant fraction of S was present in volatile species such as H_2S .
 16. D. Wooden *et al.*, *Astrophys. J.* **517**, 1034 (1999) and references therein.
 17. J. A. Nuth, N. M. Johnson, *Icarus* **180**, 243 (2006).
 18. D. Brownlee, personal communication.
 19. J. Licandro *et al.*, *Astron. Astrophys.* **398**, L45 (2003).
 20. L. A. Soderblom *et al.*, *Icarus* **167**, 100 (2004).
 21. J. K. Wilson *et al.*, *Geophys. Res. Lett.* **25**, 225 (1998).
 22. A. Toppani *et al.*, *Nature* **437**, 1121 (2005).
 23. S. Sandford, *Science* **231**, 1540 (1986).
 24. J. Bradley, personal communication.
 25. G. J. Flynn *et al.*, in *Dust in Planetary Systems*, proceedings of the conference held 26 to 28 September 2005, Kaua'i, Hawaii (Lunar and Planetary Institute Contribution No. 1280, 2005), p. 48.
 26. B. C. Clark *et al.*, *Astron. Astrophys.* **187**, 779 (1987).
 27. Also reported by M. N. Fomenkova *et al.* (54), based on the fact that F. K. Rietmeijer (55) had reported carbonates and layer silicates as minor phases in anhydrous chondritic porous IDPs.
 28. J. D. Bregman *et al.*, *Astron. Astrophys.* **187**, 616 (1987).
 29. A. Li, B. T. Draine, *Astrophys. J.*, in press.
 30. K. Tomeoka, P. R. Buseck, *Science* **231**, 1544 (1986).
 31. L. Deutsch *et al.*, *Astrophys. Space Sci.* **224**, 89 (1995).
 32. M. S. Hanner *et al.*, *Astrophys. J.* **502**, 871 (1998).
 33. D. Bockelee-Morvan *et al.*, *Icarus* **116**, 18 (1995).
 34. Y. Kimura *et al.*, *Astron. Astrophys.* **442**, 507 (2005).
 35. L. P. Keller *et al.*, *Nature* **417**, 148 (2002).
 36. L. P. Keller *et al.*, *Lunar Planet. Sci. Conf.* **XXXI**, abstract 1860 (2000).
 37. S. Hony *et al.*, *Astron. Astrophys.* **393**, L103 (2002).
 38. J. P. Bradley, in *Astrominerology*, vol. 609 of *Lecture Notes in Physics*, T. Henning, Ed. (Springer-Verlag, Berlin-Heidelberg-New York, 2002), pp. 217–235.
 39. H. Schulze, J. Kissel, *Meteoritics* **27**, 286 (1992).
 40. J. S. Sunshine *et al.*, *Science* **311**, 1453 (2006).
 41. Due to an O-H bending mode, the broad 6.0- μ m feature is similar to the broad 3- μ m water ice absorption feature. It had not been positively detected in comets before DI, although Bregman *et al.* (28) allude to a "deficit versus the best fit greybody at 6.0 μ m" in the December 1985 spectrum of comet 1P/Halley.
 42. J. Crovisier, personal communication.
 43. M. F. A'Hearn *et al.*, *Icarus* **118**, 223 (1995).
 44. C. Kemper *et al.*, *Astrophys. J.* **609**, 826 (2004).
 45. A. Cheng, *Adv. Space. Res.* **33**, 1558 (2004).
 46. A. P. Boss, *Astrophys. J.* **616**, 1265 (2004).
 47. H.-P. Gail, *Astron. Astrophys.* **413**, 571 (2004).
 48. J. A. Nuth *et al.*, *Nature* **406**, 275 (2000).
 49. S. M. Lederer, H. Campins, *Earth Moon Planets* **90**, 381 (2002).
 50. G. Sarid *et al.*, *Pub. Astron. Soc. Pacific* **117**, 796 (2005).
 51. C. Ceccarelli *et al.*, *Astron. Astrophys.* **395**, L29 (2002).
 52. A. Chiavassa *et al.*, *Astron. Astrophys.* **432**, 547 (2005).
 53. E. K. Jessberger *et al.*, *Nature* **332**, 691 (1988).
 54. M. N. Fomenkova *et al.*, *Science* **258**, 266 (1992).
 55. F. J. Rietmeijer, *Earth Planet. Sci. Lett.* **102**, 148 (1991).
 56. This paper was based on observations taken with the NASA SST, operated by the Jet Propulsion Laboratory (JPL)/CalTech, under JPL contracts 1274400 and 1274485. The authors thank S. Bajt, J. Bradley, D. Brownlee, N. Chabot, B. Clark, N. Delo-Russo, G. Flynn, W. Glaccum, C. Grady, E. Gruen, D. Harker, K. Hibbits, W. Jackson, D. Joswiak, L. Keller, D. Lauretta, A. Li, J. Nuth, W. Reach, A. Rivkin, and D. Wellnitz for valuable discussions; G. Flynn and M. Sitko for their invaluable reviews; and J. Jackson and S. Kido for their help with the graphics.

Supporting Online Material

www.sciencemag.org/cgi/content/full/1124694/DC1

SOM Text

Fig. S1

Table S1

References and Notes

6 January 2006; accepted 13 June 2006

Published online 13 July 2006;

10.1126/science.1124694

Include this information when citing this paper.

Netrins Promote Developmental and Therapeutic Angiogenesis

Brent D. Wilson,^{1,2*} Masaaki Ii,^{7*†} Kye Won Park,^{1,3*} Arminda Sulji,^{4*} Lise K. Sorensen,² Frédéric Larrieu-Lahargue,¹ Lisa D. Urness,^{1,2} Wonhee Suh,^{1,‡} Jun Asai,⁷ Gerhardus A.H. Kock,⁷ Tina Thorne,⁷ Marcy Silver,⁷ Kirk R. Thomas,^{1,5} Chi-Bin Chien,^{4,6||} Douglas W. Losordo,^{7||} Dean Y. Li^{3||}

Axonal guidance and vascular patterning share several guidance cues, including proteins in the netrin family. We demonstrate that netrins stimulate proliferation, migration, and tube formation of human endothelial cells *in vitro* and that this stimulation is independent of known netrin receptors. Suppression of *netrin1a* messenger RNA in zebrafish inhibits vascular sprouting, implying a proangiogenic role for netrins during vertebrate development. We also show that netrins accelerate neovascularization in an *in vivo* model of ischemia and that they reverse neuropathy and vasculopathy in a diabetic murine model. We propose that the attractive vascular and neural guidance functions of netrins offer a unique therapeutic potential.

Neuronal pathfinding is directed by a series of extracellular guidance cues that either attract or repulse growing axons. All of the four major families of neural guidance cues—ephrins, semaphorins, slits, and netrins—have been shown to direct patterning in the vascular system (1–4). The netrins are the prototypical axonal attractants, first identified as extracellular factors secreted from the floor plate that attract spinal commissural axons toward the midline (5). This family includes netrin-1, netrin-2 (netrin-3 in mouse), netrin-4, and the netrin-related molecules, netrin-G1 and netrin-G2.

The signaling pathways for netrin-1 are best understood. Receptors in the deleted in colo-

rectal cancer (DCC) subfamily (DCC and netogenin) mediate axon attraction toward netrin-1 (2), although this signal can be converted from an attractive to a repulsive cue by binding of netrin to the Unc5b receptor (6). The adenosine 2b receptor (A2b) reportedly binds to netrin-1 (7), but its role in netrin-mediated axonal extension has been questioned (8).

Netrins have roles that extend beyond axonal guidance. The netrins are expressed in Schwann cells, are required for regeneration and maintenance of the central nervous system (9, 10), and have been implicated in the development of mammary gland, lung, pancreas, and blood vessel (11–14). Although others have reported that

netrin-1 inhibits endothelial migration and blocks filopodial extension through the repulsive netrin receptor Unc5b (14), we have suggested that netrin-1 functions as a proangiogenic factor (13).

Netrins are endothelial mitogens and chemoattractants. To further elucidate the activity of netrins, we first evaluated the effects of purified netrin proteins on the behavior of human microvascular endothelial cells (HMVECs) *in vitro*. Netrin-1, -2, and -4 all stimulated migration of HMVECs in a dose-dependent fashion (Fig. 1), inconsistent with a published report concluding that netrin-1 inhibited migration of endothelial cells (14). To exclude the possibility of contamination in our netrin preparations, we used mass

¹Program in Human Molecular Biology and Genetics, ²Division of Cardiology, ³Department of Oncological Sciences, ⁴Department of Neurobiology and Anatomy, ⁵Division of Hematology, ⁶Brain Institute, University of Utah, Salt Lake City, UT 84112, USA. ⁷Division of Cardiovascular Research, Caritas St. Elizabeth's Medical Center, Tufts University School of Medicine, Boston, MA 02135, USA.

*These authors contributed equally to this work.

†Present address: Stem Cell Translational Research, Institute of Biomedical Research and Innovation/RIKEN Center for Developmental Biology, Kobe 650-0047, Japan.

‡Present address: Department of Medicine, Samsung Medical Center, Samsung Biomedical Research Institute, Sungkyunkwan University School of Medicine, 50 Ilwon-dong, Kangnam-Ku, Seoul 135-710, Korea.

§Present address: Department of Cardiology, Thoraxcenter, University Medical Center Groningen, University Groningen, 30.001 Groningen, Netherlands.

||To whom correspondence should be addressed. E-mail: dean.li@hmbg.utah.edu (D.Y.L.); douglas.losordo@tufts.edu (D.W.L.); chi-bin.chien@neuro.utah.edu (C.B.C.)

spectroscopy and SDS–polyacrylamide gel electrophoresis (SDS–PAGE) to show that they were >95% pure. Moreover, depletion of the media by antibody to netrin removed all promigratory activity (fig. S1). Because the previous report used conditioned media containing netrin-1 (1 $\mu\text{g/ml}$) (14), we also considered the possibility that netrin could be inhibiting an induced migratory behavior of endothelial cells. We therefore examined the effect of the netrins on vascular endothelial growth factor (VEGF)–induced migration (Fig. 1B) and found that, even at the published concentrations, netrins did not inhibit endothelial migration toward VEGF. Netrin-1, -2, and -4 were also found to stimulate endothelial proliferation and tube formation (Fig. 1, C and D) but, despite their structural similarities to the laminin family of extracellular matrix proteins, did not promote endothelial cell adhesion. The chemotactic and mitogenic effects of the netrins were reproduced in two different laboratories using similar but not identical protocols. These effects were observed on HMVECs and other endothelial cell lines, including human umbilical vein endothelial cells (HUVECs), human umbilical artery endothelial cells (HUAECs), human coronary artery endothelial cells (HCAECs), and murine endothelial cells (MS1s) (fig. S2).

Because of the suggestion that Unc5b mediates signaling by netrin-1 in the endothelium (14), we examined expression of Unc5b and the other known netrin receptors in the endothelial cell lines used in our cell biology assays (Fig. 2A). By using quantitative, real-time reverse transcription

polymerase chain reaction (RT–PCR), we detected high concentrations of the endothelial receptors roundabout 4 (Robo4), platelet endothelial cell adhesion molecule (PECAM), and VEGF receptor–2 (VEGFR-2 or Flk-1) but did not detect significant expression of Unc5b or the other known netrin receptors. Western blots using antibodies directed against DCC, neogenin, or Unc5b were similarly negative. We then used co-immunoprecipitation to test whether netrin-4 binds Unc5b and the other netrin receptors. Although netrin-1 bound as predicted to all known netrin receptors, netrin-4 did not bind to DCC, neogenin, or the Unc5 receptors (Fig. 2B and fig. S3), despite having activity similar to that of netrin-1 in endothelial cell assays and in vitro axon extension experiments (15, 16). We also revisited the possibility that A2b could serve as an endothelial netrin receptor (1, 2, 17, 18). We found that netrin-1 and netrin-4 did not bind to A2b (Fig. 2C) or stimulate A2b-mediated cyclic adenosine monophosphate (cAMP) production (Fig. 2, D and E) and that adenosine antagonists did not inhibit netrin's biologic effect (fig. S3). Together, the expression, binding, and signaling experiments indicate that the proangiogenic response of cultured human endothelial cells to netrins, especially netrin-4, is not mediated by known netrin receptors.

Zebrafish netrin1a is required for parachordal vessel formation. The effects of exogenous netrins on cultured endothelial cells led us to examine the required roles of endogenous netrin by using *fli:egfp* zebrafish embryos, whose

endothelium expresses enhanced green fluorescent protein (EGFP) (19) (Fig. 3). From <24 to 32 hours postfertilization (hpf), the netrin-1 ortholog, *netrin1a*, was expressed strongly in the ventral neural tube, weakly in the somites, and strongly in muscle pioneer cells in the horizontal myoseptum (HMS), which divides ventral from dorsal somites (20) (Fig. 3H). It was reported that injecting a translation-blocking antisense morpholino oligonucleotide (MO) at the one-cell stage leads to ectopic vascular sprouting at 48 hpf (14). In our studies, this MO caused severe defects during gastrulation at even moderate doses, suggesting a requirement for maternally transcribed *netrin1a*. To avoid these confounding defects, we used a splice-blocking MO targeting the *netrin1a* exon1–intron1 boundary, which abolished normal mRNA splicing but did not grossly affect overall trunk morphology (Fig. 3, A and B, and fig. S4). In *netrin1a* MO-injected embryos (morphants), the intersegmental vessels (ISVs) and the dorsal longitudinal anastomotic vessels (DLAVs) formed normally. However, formation of the parachordal vessels (PAVs) was strongly inhibited (Fig. 3, C and G). In *netrin1a* morphants at 50 to 54 hpf, 60% (29/48) of hemisegments lacked all *fli:egfp*-positive cells at the presumptive position of the PAV, a condition almost never seen in uninjected wild types (1%, 1/99) or control morphants (4%, 5/128). After 24 hpf, the posterior cardinal vein (PCV) normally gives rise to secondary sprouts, which grow dorsally (21) (Fig. 3, C and I) and by ~36 hpf contribute to the PAV, which becomes

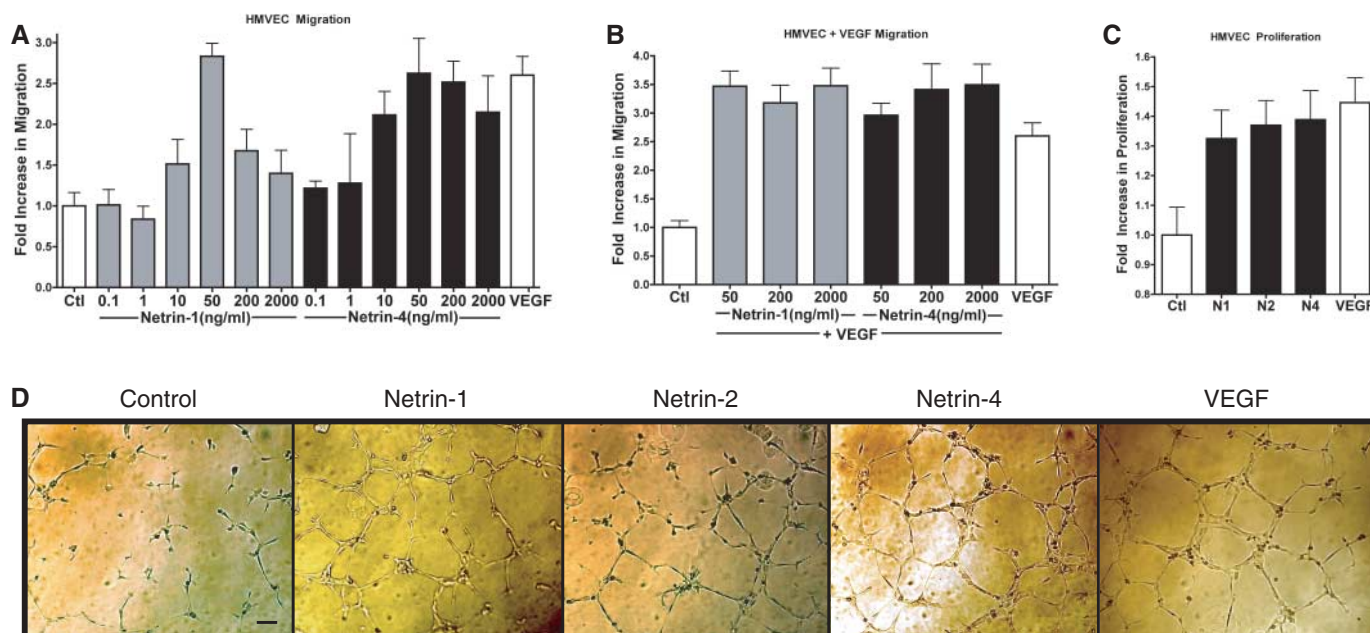


Fig. 1. Netrin function in vitro. (A) Migration of HMVECs toward netrins. Migration was measured in a Boyden chamber containing varying concentrations of netrin-1 or netrin-4 in the lower well. The number of migrating cells was normalized to a 0.1% bovine serum albumin (BSA) control (Ctl); the positive control was 13 ng/ml VEGF. Note that 50 ng/ml netrin-1 or -4 and 13 ng/ml VEGF are equimolar (0.625 nM). Bars represent mean \pm SEM of 24 separate determinations. (B) Migration of HMVECs

toward 50 to 2000 ng/ml netrin-1 and netrin-4 in the presence of 13 ng/ml VEGF. (C) Proliferation of HMVECs over 72 hours in the presence of 0.1% BSA (Ctl); 50 ng/ml netrin-1 (N1), -2 (N2), or -4 (N4); or 13 ng/ml VEGF. Number of cells is normalized to plates containing only BSA. (D) Tube formation of HUVECs stimulated by netrin-1 and -4 (200 ng/ml) as well as VEGF (13 ng/ml) compared with stimulation by control (0.1% BSA). Scale bar, 200 μm .

visible as *fli:egfp*-positive cells at the HMS, coincident with domains of strong *netrin1a* expression (21) (Fig. 3H). In *netrin1a* morphants at 36 hpf, 66% (79/120) of hemisegments lacked *fli:egfp*-positive cells at the HMS, which was never seen in uninjected controls (0/115). Secondary sprouts from the PCV seemed to form normally in *netrin1a* morphants at 36 hpf (Fig. 3D); at 50 hpf, secondary sprouts at the HMS occasionally extended ectopic projections as though searching to form a PAV (Fig. 3G) (14). The absence of PAVs in *netrin1a* morphants, together with the strong expression of *netrin1a* messenger RNA (mRNA) by muscle pioneers that prefigures the PAV, are most consistent with a proangiogenic role for *netrin1a*.

Netrins promote neovascularization in mammalian models. The cell biology and zebrafish data led us to hypothesize that netrins could induce neovascularization in vivo. We therefore compared netrins with VEGF in their ability to promote angiogenesis and reperfusion in a murine model of hindlimb ischemia (22). The iliac artery of FVB/NJ mice was ligated, resulting in severe vascular perfusion defects. Blood flow was measured with laser Doppler imaging and quantitated as the ratio of ischemic to nonischemic limbs. Expression of netrin-1, netrin-4, and VEGF complementary DNA molecules (cDNAs) was driven by a cytomegalovirus (CMV) enhancer and a Rous sarcoma virus (RSV) promoter that were characterized previously in preclinical and clinical trials of VEGF (23–27). The base expression vector (empty vector) was used as a control. All constructs were delivered locally into the ischemic gastrocnemius muscle at 0, 7, 14, and 21 days after induction of ischemia. Imaging revealed that hindlimb perfusion was significantly improved 7 days postsurgery in mice injected with netrin-1, netrin-4, or VEGF constructs compared with those of mice injected with empty vector (Fig. 4A). Serial Doppler measurements demonstrated continued improvement in limb perfusion, with the greatest effect at 28 days after induction of ischemia. Histological analysis after day 28 showed a significantly greater (>twofold) capillary density and reduced fibrosis in the netrin-1-, netrin-4- and VEGF-treated animals (fig. S5). Interestingly, more vessels stained positive for smooth muscle α -actin in netrin-1-treated animals than in netrin-4- or VEGF-treated animals, suggesting a greater number of vessels with medial layers.

The dual role of netrin in guiding nerves and blood vessels suggests that netrins may have unique therapeutic potential. In diabetes and related metabolic syndromes, neural and vascular compromise appear together clinically (28, 29). Reduced nerve conduction velocity is an early marker of neuropathy in diabetic models, such as *db/db* mice, and is secondary to a combination of pathologic effects on neuronal cells and compromise to perineural vascular beds (vasa nervosa). To examine whether netrins reverse diabetic vasculopathy and neuropathy in *db/db*

mice, we delivered netrin-1 and netrin-4 expression constructs into their hindlimbs every 7 days for a total of 28 days. After 7 days of treatment with vectors expressing netrin-1, netrin-4, or VEGF, both motor and sensory sciatic nerve conduction velocities in *db/db* mice returned to nondiabetic amounts and were significantly better than empty vector-injected controls (Fig. 4). At 14 days, the conduction velocities in netrin-1-treated mice continued to improve beyond nondiabetic values, whereas those measured in either netrin-4- or VEGF-treated animals remained near normal nondiabetic conduction ve-

locities. The improvement in conduction velocities in *db/db* mice treated with netrin-1, netrin-4, or VEGF was associated with increased capillary density of the vasa nervosa surrounding the sciatic nerve (fig. S6). The increased capillary density was correlated with endothelial proliferation as measured by 5-bromo-2'-deoxyuridine (BrdU) incorporation and lectin staining. The amounts of endothelial proliferation in netrin-1-, netrin-4-, and VEGF-treated animals were similar, although animals exposed to netrin-1-containing vectors showed proliferation of cells that also expressed the Schwann cell marker

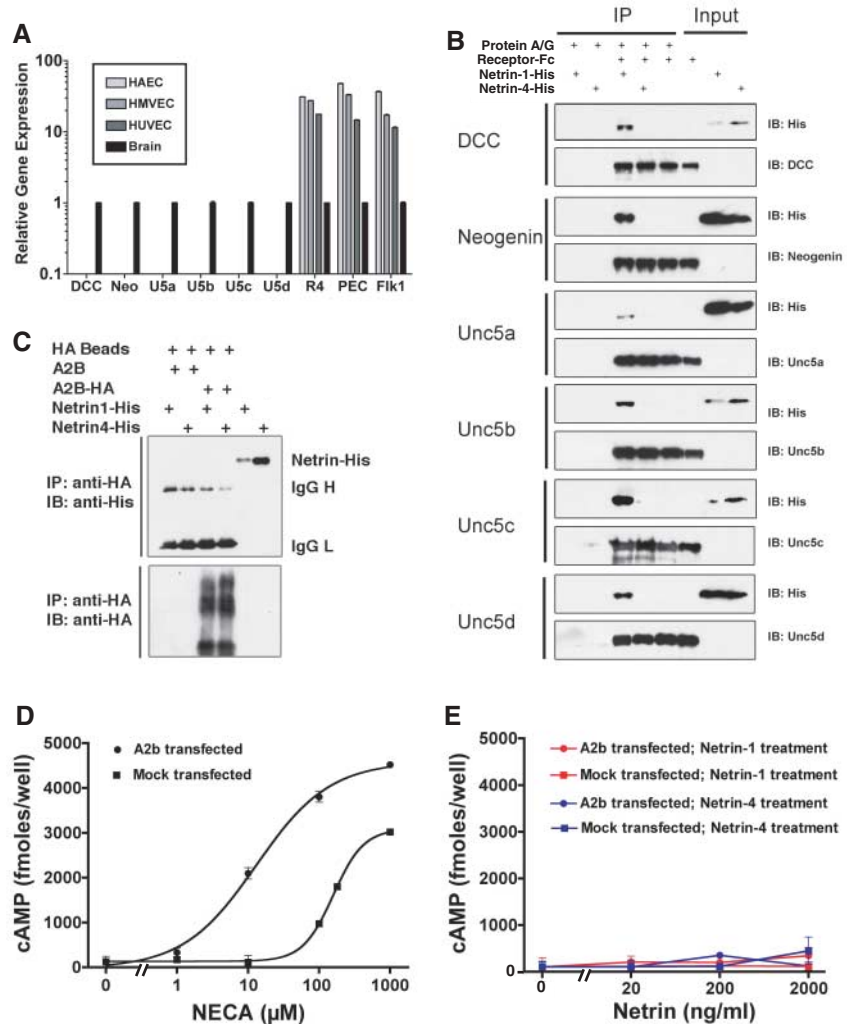


Fig. 2. Angiogenic effects of netrin-1 and netrin-4 are not mediated by known or postulated netrin receptors. (A) Quantitative real-time RT-PCR of DCC receptors (DCC and neogenin), Unc5 receptors (U5a to U5d), Robo4 (R4), PECAM (PEC), and VEGF receptor (Flk1). Expression amounts were measured relative to that of glyceraldehyde-3-phosphate dehydrogenase (GAPDH) and compared with transcript amounts in brain tissue (normalized to 1). The absence of bars indicates values less than 0.1. (B) Co-immunoprecipitation (co-IP) of purified receptor-Fc fusion proteins (N-terminal) and 10X-His-tagged netrin proteins (C-terminal). Immunoblotting (IB) performed with antibody to His or receptor-specific antibody. (C) Co-IP of purified netrin-1-His and netrin-4-His incubated with lysates of A2b-hemagglutinin (HA)-transfected human embryonic kidney (HEK) 293T cells. Precipitation and immunoblot were carried out by using antibodies against HA and His, respectively. (D and E) Stimulation of cAMP accumulation by 5'-(N-ethylcarboxamido) adenosine (NECA) and netrins. HEK cells were transfected with vectors expressing A2b or the G protein-coupled receptor, arginine vasopressin receptor-2 (mock), and exposed to increasing concentrations of NECA (D) or netrin-1 or netrin-4 (E). Error bars indicate SEM.

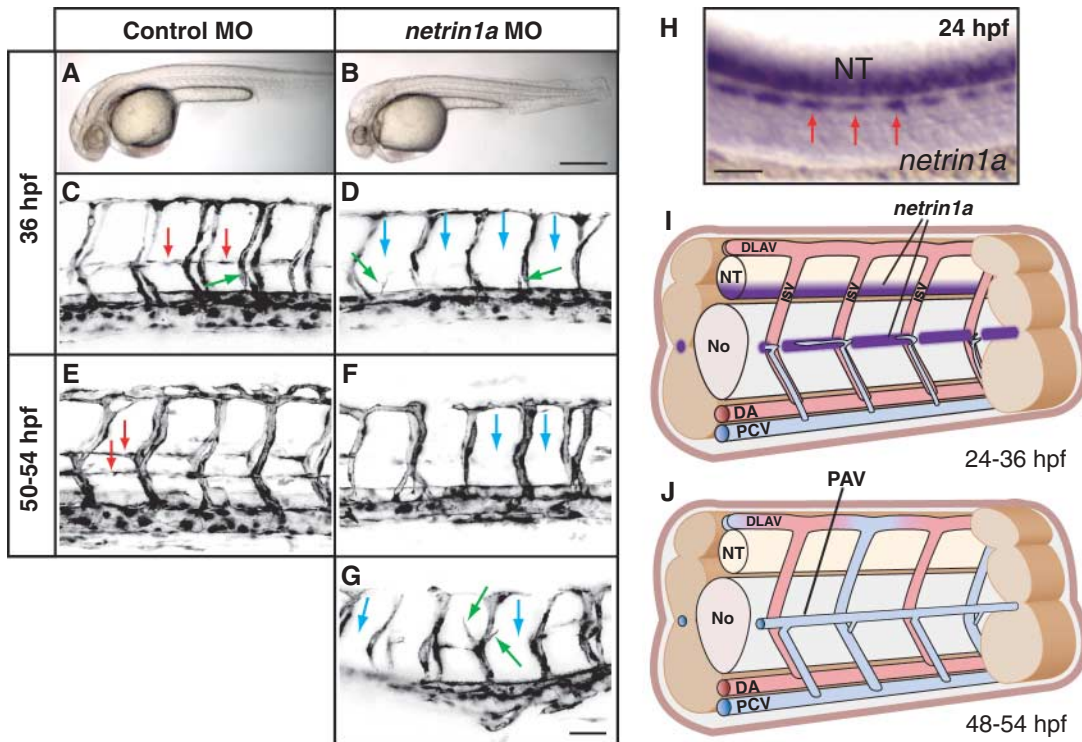


Fig. 3. Knockdown of zebrafish *netrin1a* prevents formation of a specific vessel, the PAV. *fli:egfp* zebrafish embryos were injected at the one- to two-cell stage with a control MO or a splice-blocking *netrin1a* MO and analyzed at 36 to 54 hpf. (A and B) Brightfield images. Scale bar, 400 μ m. (C to G) Confocal projections showing lateral views of somites 7 to 11; anterior to the left. Embryo in (E) is tilted to visualize both sides. Red arrows indicate PAV in control embryos; blue arrows indicate absence of PAVs in morphants; green arrows indicate secondary sprouts growing dorsally from the PCV in controls and morphants. Scale bar, 50 μ m. (G) Secondary sprouts occasionally give rise to short branches at the presumptive location of the PAV (green arrows). (H) In situ hybridization for *netrin1a* shows strong staining at the HMS (red arrows). 24 hpf, lateral view of somites 7 to

14. Scale bar, 50 μ m. NT, neural tube. (I) Schematic, 24 to 36 hpf. *Netrin1a* is expressed at the horizontal myoseptum through 32 hpf; weak expression in somites not shown. By 36 hpf, secondary sprouts (blue) arise from the PCV and begin to form the PAV at the myoseptum. DA, dorsal aorta; No, notochord. (J) Schematic, 48 to 54 hpf. By this time, ISVs have started to acquire arterial or venous fates. The PAV is mature and connected to the veins by shunts. Without *netrin1a* function, the PAV does not form.

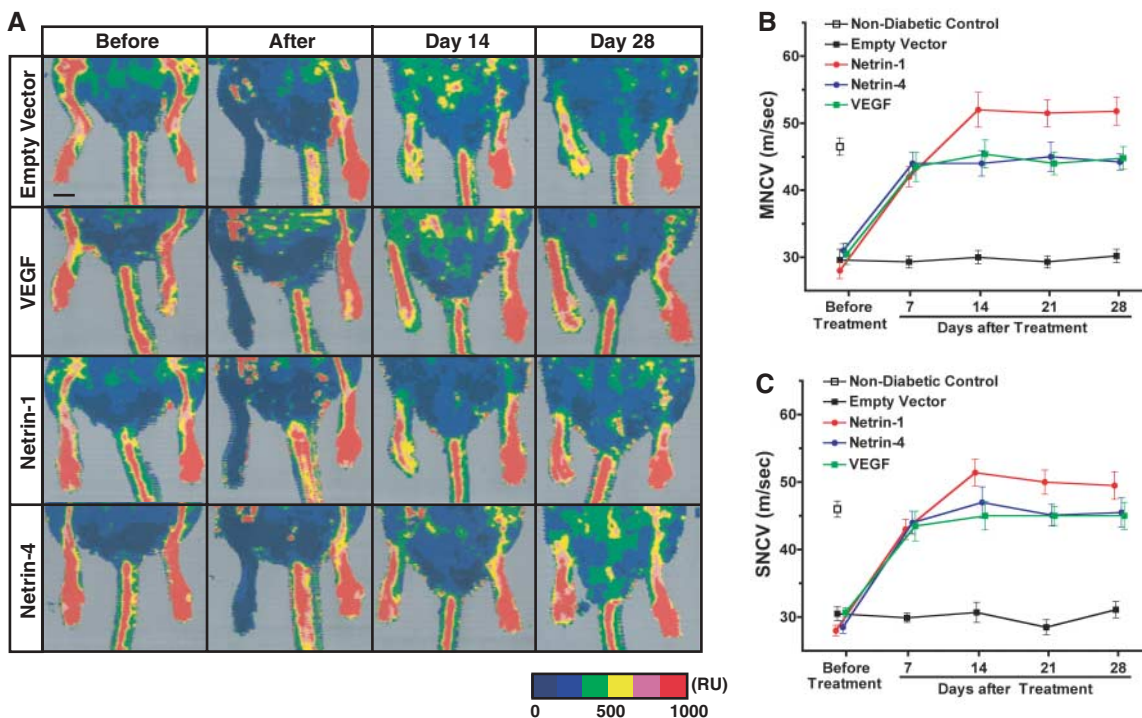


Fig. 4. Local delivery of VEGF, netrin-1, or netrin-4 expression constructs promotes revascularization and restoration of nerve conduction velocity. (A) Hindlimb ischemia was surgically induced in FVB/NJ mice by ligation and excision of the proximal femoral artery as described previously (22). VEGF, netrin-1, netrin-4, and empty vector DNA expression plasmids (50 μ g of DNA in 100 μ l of saline in each group) were locally injected into the right gastrocnemius muscle immediately, 7, 14, and 21 days after surgery. Laser Doppler perfusion imaging was used to record serial blood flow measurements over the course of 4 weeks post-operatively, as previously described (32). In these digital color-coded images,

red indicates regions with maximum perfusion, yellow depicts medium perfusion, and blue identifies low perfusion. Scale bar, 3 mm. Color bar in lower right corner displays absolute values in readable units (RU). (B) Motor nerve conduction velocities (MNCVs) in *db/db* mice 7 days after injection with VEGF, netrin-1, or netrin-4. (C) Sensory nerve conduction velocities (SNCVs) in *db/db* mice 7 days after injection with VEGF, netrin-1 (NT1), netrin-4 (NT4), or empty vector constructs. Uninjected, nondiabetic mice serve as controls in both (B) and (C). Error bars indicate SEM.

S100. These data suggest that netrin-1 reverses vascular and neural pathology in *db/db* mice by stimulating both endothelial and Schwann cells and may account for the superior recovery of nerve conduction seen in netrin-1-treated *db/db* mice.

Conclusion. By using zebrafish and mammalian systems, loss-of-function and gain-of-function strategies, and in vivo and in vitro assays, we have shown that netrins stimulate angiogenesis. First, netrin-1, -2, and -4 induce migration, proliferation, and tube formation in multiple endothelial cell lines. Surprisingly, we could identify none of the known netrin receptors as being responsible for these behaviors. Second, the inhibition of *netrin1a* mRNA in zebrafish reveals a requirement for netrin signaling in formation of PAVs. Lastly, netrins can activate blood vessel formation and accelerate revascularization and reperfusion of ischemic tissue in two murine disease models.

It has been proposed that netrin signaling in the vasculature can be mediated by the repulsive Unc5b receptor and that the experimental attenuation of either netrins or Unc5b results in increased branching of vessels in zebrafish and mice (14). However, we could not detect significant amounts of Unc5b in any of the responsive cell lines, nor could we detect any binding of Unc5b to netrin-4, despite the fact that netrin-4 elicits an endothelial response identical to that of netrin-1 in all of our in vitro and in vivo assays. Moreover, we were unable to find any evidence that netrins can inhibit vascular growth in vivo. Knocking down *netrin1a* mRNA in zebrafish by using a splice-blocking MO prevents formation of the PAV, implying a proangiogenic role. PAVs are absent in both *netrin1a* and *unc5b* morphants in the published work of others [figure 2 of Lu *et al.* (14)]. These authors did not remark upon these findings and focused on ectopic sprouting in their morphants at 48 hpf. We also observed ectopic sprouting, but this occurred in a minority of *netrin1a* morphants and appeared secondary to loss of the PAV at 36 hpf. The temporal sequence of events during zebrafish embryogenesis is most consistent with a role of netrin as a positive regulator of angiogenesis. We also generated mice carrying a targeted deletion of exons 4 to 13 of the Unc5b locus (figs. S7 and S8). Embryos homozygous for this mutation show normal branching of cranial, intersomitic, hindbrain, and yolk sac vessels; whether this is due to allelic difference or strain background (shown to modify the Unc5b phenotype) is currently under investigation.

The ability of netrins to promote the growth of both neurons and vasculature has made them a promising therapeutic target for treating a number of degenerative diseases. Our studies demonstrate that netrins promote neovascularization and reperfusion in a murine model of peripheral vascular disease. In fact, vectors expressing netrin-1 and netrin-4 are comparable in effectiveness to vectors expressing VEGF that

are currently being tested in phase II clinical trials. A potential advantage of netrin-1 over VEGF is that it enhances capillary density and stimulates smooth muscle cells to form a vascular media in both in vitro (13) and in vivo studies (fig. S5). Microvascular disease and polyneuropathy are morbid complications of long-standing diabetes whose onset is delayed but not prevented by intensive blood glucose control with insulin or oral agents (30, 31). Here, we show that the netrins restore nerve function and vascular supply in a murine model of diabetes. Although netrin-1 has proangiogenic effects similar to those of VEGF and netrin-4 in this model, our data suggest that netrin-1 is superior in restoring nerve conduction velocity, possibly because it has potent effects on both endothelial and neural biology. This report provides proof of concept for a novel therapeutic strategy aimed at using the dual vascular and neural regenerative properties of guidance molecules to treat diabetic complications that result from vasculopathy and neuropathy and sets the stage for further investigation.

References and Notes

1. M. Klagsbrun, A. Eichmann, *Cytokine Growth Factor Rev.* **16**, 535 (2005).
2. P. Carmeliet, M. Tessier-Lavigne, *Nature* **436**, 193 (2005).
3. A. Eichmann, F. Le Noble, M. Autiero, P. Carmeliet, *Curr. Opin. Neurobiol.* **15**, 108 (2005).
4. B. M. Weinstein, *Cell* **120**, 299 (2005).
5. T. Serafini *et al.*, *Cell* **78**, 409 (1994).
6. K. Hong *et al.*, *Cell* **97**, 927 (1999).
7. V. Corset *et al.*, *Nature* **407**, 747 (2000).
8. E. Stein, Y. Zou, M.-m. Poo, M. Tessier-Lavigne, *Science* **291**, 1976 (2001).
9. F. Cebria, P. A. Newmark, *Development* **132**, 3691 (2005).
10. R. D. Madison, A. Zomorodi, G. A. Robinson, *Exp. Neurol.* **161**, 563 (2000).
11. K. Srinivasan, P. Strickland, A. Valdes, G. C. Shin, L. Hinck, *Dev. Cell* **4**, 371 (2003).
12. M. Yebra *et al.*, *Dev. Cell* **5**, 695 (2003).

13. K. W. Park *et al.*, *Proc. Natl. Acad. Sci. U.S.A.* **101**, 16210 (2004).
14. X. Lu *et al.*, *Nature* **432**, 179 (2004).
15. Y. Yin, J. R. Sanes, J. H. Miner, *Mech. Dev.* **96**, 115 (2000).
16. M. Koch *et al.*, *J. Cell Biol.* **151**, 221 (2000).
17. H. Arakawa, *Nat. Rev. Cancer* **4**, 978 (2004).
18. P. Mehlen, C. Furne, *Cell. Mol. Life Sci.* **62**, 2599 (2005).
19. N. D. Lawson, B. M. Weinstein, *Dev. Biol.* **248**, 307 (2002).
20. J. D. Lauderdale, N. M. Davis, J. Y. Kuwada, *Mol. Cell. Neurosci.* **9**, 293 (1997).
21. S. Isogai, N. D. Lawson, S. Torrealday, M. Horiguchi, B. M. Weinstein, *Development* **130**, 5281 (2003).
22. T. Couffinhal *et al.*, *Am. J. Pathol.* **152**, 1667 (1998).
23. A. Kawamoto *et al.*, *Circulation* **110**, 1398 (2004).
24. J. P. Reilly *et al.*, *J. Interv. Cardiol.* **18**, 27 (2005).
25. P. Schratzberger *et al.*, *J. Clin. Investig.* **107**, 1083 (2001).
26. D. W. Losordo *et al.*, *Circulation* **105**, 2012 (2002).
27. D. H. Walter *et al.*, *Circulation* **110**, 36 (2004).
28. M. Li *et al.*, *Circulation* **112**, 93 (2005).
29. Y. S. Yoon *et al.*, *Circulation* **111**, 2073 (2005).
30. Diabetes Control and Complications Trial Research Group, *Ann. Intern. Med.* **122**, 561 (1995).
31. UK Prospective Diabetes Study Group, *Lancet* **352**, 837 (1998).
32. T. Murohara *et al.*, *J. Clin. Investig.* **101**, 2567 (1998).
33. We thank K. Whitehead, P. Lindblom, and H. Gerhardt for technical expertise and assistance; I. Shepherd, L. Hinck, and D. Grunwald for reagents; the Mass Spectroscopy Core Facility at the University of Utah; and D. Lim for graphics. D.Y.L. is supported by grants from NIH, American Cancer Society, American Heart Association (AHA), Flight Attendants Medical Research Institute, and Burroughs Wellcome Fund. C.B.C. is supported by grants from NIH. D.W.L. is supported by grants from NIH and AHA. B.D.W. is an American College of Cardiology Foundation/Pfizer Fellow in Cardiovascular Medicine.

Supporting Online Material

www.sciencemag.org/cgi/content/full/1124704/DC1

Materials and Methods

SOM Text

Figs. S1 to S8

6 January 2006; accepted 23 May 2006

Published online 29 June 2006;

10.1126/science.1124704

Include this information when citing this paper.

The *Neurospora* Checkpoint Kinase 2: A Regulatory Link Between the Circadian and Cell Cycles

Antônio M. Pogueiro,¹ Qiuyun Liu,³ Christopher L. Baker,¹ Jay C. Dunlap,^{1*} Jennifer J. Loros^{1,2*}

The clock gene *period-4* (*prd-4*) in *Neurospora* was identified by a single allele displaying shortened circadian period and altered temperature compensation. Positional cloning followed by functional tests show that PRD-4 is an ortholog of mammalian *checkpoint kinase 2* (*Chk2*). Expression of *prd-4* is regulated by the circadian clock and, reciprocally, PRD-4 physically interacts with the clock component FRQ, promoting its phosphorylation. DNA-damaging agents can reset the clock in a manner that depends on time of day, and this resetting is dependent on PRD-4. Thus, *prd-4*, the *Neurospora Chk2*, identifies a molecular link that feeds back conditionally from circadian output to input and the cell cycle.

Many core components of cellular circadian clocks constitute molecular feedback loops (1–4). Additional circuits, although not required for circadian function, can

connect the clock to its outputs or even feed back to affect the core loops or input to them (5–7). In mammals, one prominent circadian output leads to regulation of the cell cycle (8–10).